ever, there are not any data for a shorter wavelength AlGaInP laser diode with real-index waveguide using a AlInP current blocking layer.

In this paper, we believe we report a real-index-guided 630-nm-band AlGaInP laser diode with AlInP current blocking layer for the first time.

The schematic structure is shown in Fig. 1. The device has a buried-ridge stripe structure with $Al_{0.5}In_{0.5}P$ current blocking layer, which is transparent for the wavelength of the 630-nm-band and has a smaller refractive index (3.280 for 635 nm) than that (3.345 for 635 nm) of the $(al_{0.7}Ga_{0.3})_{0.5}In_{0.5}P$ cladding layer. The active layer is the strain-compensated multiple quantum well structure (SC-MQW)^2 with the tensile strained quantum wells (-1.1%, 100 Å) and compressively strained barriers.

Figure 2 shows the I-L characteristics for the real-index-guided laser diode with AlInP current blocking layer and the loss-guided laser diode with GaAs current blocking layer. The threshold current and the slope efficiency for the real-index-guided laser diode with a cavity length of 400 μm were 20 mA and 0.5 W/A, respectively. These characteristics are superior to those of the loss-guided laser diodes. This improvement in the threshold current and the slope efficiency is due to a reduction in the optical absorption of the laser beam at the current blocking layer. This laser diode is lasing at 638 nm.

Figure 3 shows the temperature dependence of the I-L characteristics for the real-index-guided laser diode. The maximum operating temperature is 95°C. This laser diode has operated reliably for more than 1000 h at 60°C under 5 mW.
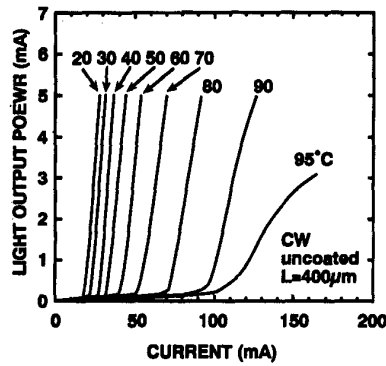
In summary, we successfully fabri-
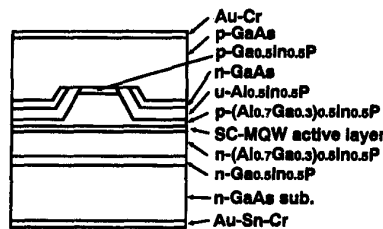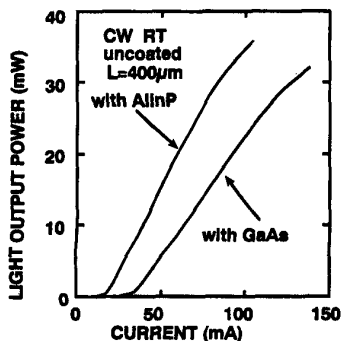
CThP6   Fig. 3   Temperature dependence of I-L characteristics.

cated real-index-guided 630-nm-band AlGaInP laser diodes for the first time, to our knowledge. A threshold current of 20 mA and slope efficiency of 0.5 W/A were achieved.
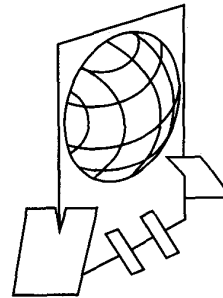
1. R. Kobayashi, et al., IEEE J. Sel. Top. Quantum Electron. 1, 723 (1995).
2. R. Hiroyama, et al., 14th Semiconductor Laser Conference, paper W3.5.

CThQ   2:30 pm
                                 Salon F

Fabrication of Microstructures

Milan R. Kokta, Union Carbide Corporation, Presider

CThQ1   **2:30 pm**

Out-of-plane refractive microlens for free-space integrated optics

C. R. King, L. Y. Lin, M. C. Wu, UCLA, Electrical Engineering Department, 66-147D Engineering IV, Box 951594, Los Angeles, California 90095-1594

Free-space micro-optical systems integrated on a single chip have many applications in optical data storage, sensing, communication networks, display, and packaging of optoelectronic devices. Previously, we have demonstrated a surface-micromachined "free-space micro-optical bench," which can monolithically integrate free-space micro-optical elements with active optoelectronic elements.[1] Out-of-plane micro-Fresnel lenses have been realized by this technique. Though excellent optical performance has been obtained, the Fresnel lens is a diffractive optical element and suffers from low efficiency. A refractive spherical microlens is desired for high-performance optical systems. In this paper, we report the first fabrication of an out-of-plane spherical microlens mounted on a surface-micromachined supporting plate. The focusing and collimating properties of the lens are successfully demonstrated.

The schematic diagram and the scan-

ning electron micrograph (SEM) of the out-of-plane spherical microlens are shown in Fig. 1. The microlens is fabricated on a support plate with surface-micromachined microhinges. The fabrication processes for the support plate are described in detail in Ref. 1. Before releasing the support plate, two thick layers of photoresist are applied to the substrate, and 300-μm-diameter circular patterns are exposed and developed so that the only remaining photoresist is in the form of cylinders over the support plates. The chip containing the structures is then heated to 200°C for 20 min to reflow the photoresist into a spherical surface profile.[2] After application of the microlens, the sacrificial layers for the support plate is selectively removed, and the support plate is rotated out of the plane of the wafer. A surface profile of the lens on the plate, measured by a Tencor Alpha-Step 200 profilometer, is shown in Fig. 2. The radius of curvature as calculated from the lens diameter and sag height is $R_c = 406$ μm. The maximum deviation from the spherical shape is be-
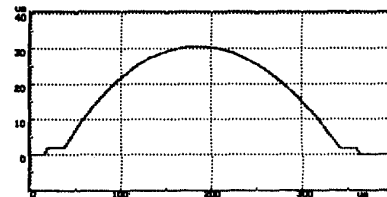

a)

b)

CThQ1   Fig. 1   (a) Schematic diagram and (b) SEM micrograph of an out-of-plane spherical microlens standing perpendicular to the substrate.

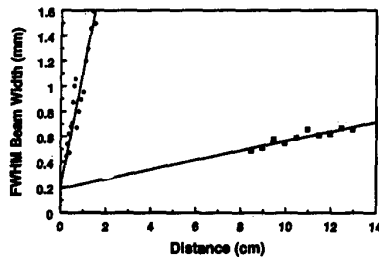**CThQ1   Fig. 2**   Surface profile of the microlens mounted on polysilicon supporting plate.

CThP6   Fig. 1   Schematic structure.

CThP6   Fig. 2   I-L characteristics.

CThQ1 Fig. 3 Beamwidth of light emitted from optical fiber both with and without the light passing through the microlens, as a function of distance from the lens.

low 0.5 μm for all areas within 5 μm from the edges.

The microlens is used to collimate a diverging optical beam from a single-mode optical fiber at λ = 633 nm. The fiber is parallel to the substrate, with the tip of the fiber positioned at one focal length from the microlens. The full width at half maximum (FWHM) of the beam, with and without passing through the microlens, is plotted against distance in Fig. 3. The beam diverges at an angle of 3.1° without the lens, and is collimated to 0.15° by the microlens.

The microlens is also used to focus a collimated beam from a 633-nm HeNe laser, using a microscope-mounted CCD. By focusing on the lens and measuring the distance of travel for the microscope objective to reach the focal point, the focal length of the lens was measured to be 645 μm.

In summary, we believe an out-of-plane spherical microlens standing perpendicular to the substrate has been demonstrated for the first time using surface-micromachining technology. Light emitted from an optical fiber is successfully collimated by the microlens to a divergence angle of 0.15°, and the focal length is measured to be 645 μm. These microlenses can be combined with other out-of-plane micro-optical components on a silicon substrate to form a free-space micro-optical bench.

1. L. Y. Lin, S. S. Lee, K. S. J. Pister, M. C. Wu, Photon. Technol. Lett. **6**, 1445 (1994).
2. T. R. Jay, M. B. Stern, R. E. Knowlden, Proc. SPIE **1751**, 236–45 (1992).

CThQ2   2:45 pm

Surface-emitting microlensed LED and its self-focusing effect
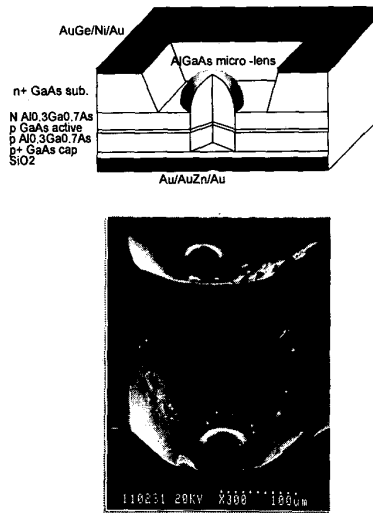
O-Seung Yang, Song-Cheol Hong, Young-Se Kwon, *Department of Electrical Engineering, Korea Advanced Institute of Science and Technology, 373-1, Kusong-Dong, Yusong-Gu, Taejon, Korea*

There have been lots of efforts to make beam patterns of LD and LED narrow in the field of optoelectronics and fiber optics. Surface-emitting (SE) diodes have been also attracting many interests due to
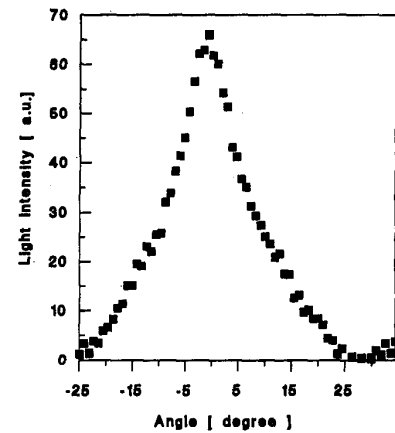
their potentiality in optical communications, optical interconnects, optical processing, etc. Integrating of light-emitting devices with microlens decreases the beam divergence, which reduces the tolerance in packaging and alignment, and couple significantly more power into fibers.[1]

GaAs/AlGaAs backside-emitting microlensed LEDs have been fabricated. Monolithic integration of AlGaAs microlens and conventional LED has been realized by meltback etching of hemisphere and subsequent regrowth of AlGaAs lens layer by liquid phase epitaxy (LPE). Fig-


CThQ2 Fig. 1 The structure of fabricated microlensed LED and the scanning electron micrograph (SEM), 30-μm radius microlens.

ure 1 shows the structure of fabricated microlensed LED and the scanning electron micrograph (SEM) of 30-μm radius AlGaAs microlens nested at the bottom inside the Burrus hole. Selective meltback of n^+ GaAs substrate produces hemispherical craters in the circular mask opening regions. No anisotropic crystal plane emerges for more than m_{Al} = 3.93 mg/1 g Ga.[2] Consecutive growth of Al-GaAs lens layer fills up the hemispherical craters to provide AlGaAs microlens. Completing the fabrication process of conventional surface-emitting LEDs, we preferentially etched out GaAs substrate from the backside by $NH_4OH:H_2O_2$ = 1:30 etching solution to expose the AlGaAs microlens surface into the air. Front-to-back infrared aligner is used in the Burrus hole-buried microlens alignment. AlGaAs microlens of 30-μm diameter diminishes the full width at half maximum (FWHM) of far-field pattern (FFP) of LED

CThQ2 Fig. 2 Far-field pattern (FFP) of fabricated microlensed LED.
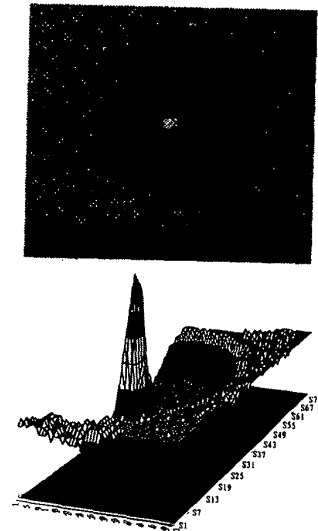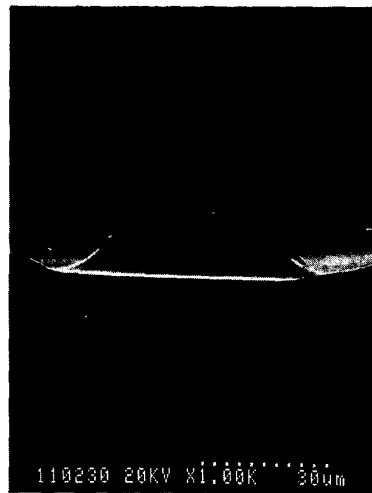
CThQ2 Fig. 3 The performance of microlens: (a) SEM of 30-μm radius microlens; (b) focused infrared (IR) image on the focal plane and 3-D diagram of IR image.